

# Mononuclear Cu(II), Zn(II), and Co(II) Complexes with 2-Furoate Anions and 2,2'-Bpy: Synthesis, Structure, and Biological Activity

I. A. Lutsenko<sup>a</sup> \*, D. S. Yambulatov<sup>a</sup>, M. A. Kiskin<sup>a</sup>, Yu. V. Nelyubina<sup>b</sup>, P. V. Primakov<sup>b</sup>, O. B. Bekker<sup>c</sup>,  
A. A. Sidorov<sup>a</sup>, and I. L. Eremenko<sup>a</sup>

<sup>a</sup>Kurnakov Institute of General and Inorganic Chemistry, Russian Academy of Sciences, Moscow, 119991 Russia

<sup>b</sup>Nesmeyanov Institute of Organoelement Compounds, Russian Academy of Sciences, Moscow, 119991 Russia

<sup>c</sup>Vavilov Institute of General Genetics, Russian Academy of Sciences, Moscow, 119991 Russia

\*e-mail: irinalu05@rambler.ru

Received April 1, 2020; revised April 8, 2020; accepted April 22, 2020

**Abstract**—The mononuclear complexes  $[M(\text{Fur})_2(\text{Bpy})(\text{H}_2\text{O})]$  ( $M = \text{Cu (I)}, \text{Zn (II)}$ ) were prepared by the reactions of copper(II) and zinc(II) acetates with 2-furoic acid (HFur) anion and 2,2'-bipyridine (Bpy) in acetonitrile. A similar reaction with  $\text{ZnCl}_2$  used instead of  $\text{Zn}(\text{OAc})_2 \cdot 2\text{H}_2\text{O}$  gave the complex  $[\text{Zn}(\text{Fur})_2(\text{Bpy})]$  (III). The cobalt(II) complex  $[\text{Co}(\text{Fur})_2(\text{Bpy})]$  (IV) was obtained by the reaction of cobalt trimethylacetate with HFur and Bpy. The structure of mononuclear complexes was determined by X-ray diffraction (CIF files CCDC nos. 1993168 (I), 1993169 (II), 1993170 (III), and 1993171 (IV)). Compounds I, III, and IV were studied for the biological activity *in vitro* against the nonpathogenic mycobacterial strain *Mycolicibacterium smegmatis*. It was found that I and III have high biological activity and are promising for further studies for antituberculosis activity.

**Keywords:** copper(II), zinc(II), and cobalt(II) complexes, 2-furoic acid, 2,2'-bipyridine, structure, biological activity

**DOI:** 10.1134/S1070328420120040

## INTRODUCTION

It is known that medicinal drugs used in clinical practice often contain coordination compounds of various metal ions [1–4]. For example, drugs based on platinum(II) derivatives (e.g., cisplatin and its analogues) are used for the therapy of cancer, while iron derivatives are employed to treat anemia. There are quite a few drugs that contain zinc, mercury, silver, and other metal ions possessing antiseptic properties [4, 5]. Therefore, the use of metal complexes as drug components is not unusual.

One trend of antituberculosis studies is related to the search for new biologically active molecules for overcoming drug resistance of *Mycobacterium tuberculosis* in the treatment of tuberculosis, a menace to humans [6]. The development of cross-drug resistance, in addition to the growth of the natural antibiotic resistance of mycobacteria (MT), propagation of the bacterial population in the dormant state, and HIV-associated tuberculosis generate global obstacles to the therapy of tuberculosis. Currently, it is generally accepted that the use of metal complexes in medicinal chemistry may help to solve many challenges associated with drug development. This approach has already proved to be efficient in the treatment of cancer, malaria, toxoplasmosis, and other dangerous dis-

eases (cisplatin, auranoftin, carboplatin, nitroprusside, silver sulfadiazine) [7–15]. Complexes with essential metals and pharmaceutical compositions based on them may become highly efficient antituberculosis drug candidates. A known factor affecting the survival and reactivation of dormant mycobacteria is the state of their redox homeostasis, which depends on the intracellular concentration of transition metal ions:  $\text{Co}^{2+}$ ,  $\text{Ni}^{2+}$ ,  $\text{Mn}^{2+}$ ,  $\text{Fe}^{3+}$ ,  $\text{Zn}^{2+}$ ,  $\text{Cu}^{2+}$ , etc. In living organisms, metals occur in various enzyme systems (peroxidases, amylases, dehydrogenases) and perform important regulatory functions (oxygen transport, redox function) [16]. This means that the designed coordination compounds are of interest as subjects for studying the activity against multiple-drug resistant and sensitive MT strains and also dormant and latent mycobacteria. 2-Furoic acid (furan-2-carboxylic acid, HFur) and its derivatives are promising organic molecules, which form the basis of several antibacterial agents such as furazolidone, furadonin, quinifuril, etc. In particular, 5-nitro-2-furoic acid derivatives inhibit the enzyme isocitrate lyase, which may account for the mechanism of their antituberculosis activity [17]. Recently, S. Melnic and co-workers demonstrated that the heterometallic triangular  $\{\text{Fe}_2\text{Co}\}$  complexes with 2-furoate anion exhibit activity *in vitro* against

*Mycobacterium tuberculosis* H37Rv [18]. Previously, we prepared zinc complexes with pyridine and 4-phenylpyridine, which showed activity in vitro against the nonpathogenic *M. smegmatis* strain used to model *M. tuberculosis* [19]. This study continues the search for efficient *d*-metal complexes based on HFur and N-donor ligands. Here we report the synthesis, structure determination, and biological activity assay for mononuclear  $\text{Cu}^{2+}$ ,  $\text{Zn}^{2+}$ , and  $\text{Co}^{2+}$  furoate complexes with 2,2'-bipyridine (Bpy).

## EXPERIMENTAL

The complexes were synthesized using commercial chemicals and solvents, which were used as received: zinc(II) acetate dihydrate (98%, Acros), zinc chloride (98% Alfa Aesar), copper(II) acetate monohydrate (95%, Acros), 2-furoic acid (Acros), acetonitrile (special purity grade, Khimmed), and 2,2'-bipyridine (Alfa Aesar). Anhydrous cobalt(II) trimethylacetate was prepared from pivalic acid (HPiv, Acros) and cobalt(II) acetate tetrahydrate (98%, Acros).

Attenuated total reflectance (ATR) IR spectra were measured on a Perkin-Elmer Spectrum 65 FT IR spectrometer in the frequency range of 400–4000  $\text{cm}^{-1}$ .

Elemental analysis was carried out on a Carlo Erba EA 1108 automated C,H,N-analyzer.

The biological activity was determined using the *M. smegmatis* mc<sup>2</sup> 155 test system with paper discs. The test included determination of the growth inhibition zone for the bacterial strain lawn-inoculated on an agarized medium around paper discs containing the test compound in various concentrations. The bacteria washed away from Petri dishes with the M-290 tryptone soya agar medium (Himedia) were grown overnight in the Lemco-TW liquid medium (Lab Lemco' Powder, 5 g  $\text{L}^{-1}$  (Oxoid); Peptone special, 5 g  $\text{L}^{-1}$  (Oxoid); NaCl, 5 g  $\text{L}^{-1}$ ; and Tween-80) at 37°C, up to the mid logarithmic growth phase at the optical density OD600 = 1.5, and then mixed with the molten M-290 agar in 1 : 9 : 10 ratio (culture : Lemco-TW : M-290). The culture was incubated for 24 h at 37°C. The compound concentration producing the minimum visible growth inhibition zone was taken as the minimum inhibitory concentration (MIC).

**Synthesis of  $[\text{Cu}(\text{Fur})_2(\text{Bpy})(\text{H}_2\text{O})]$  (I).** Weighed portions of  $\text{Cu}(\text{OAc})_2 \cdot \text{H}_2\text{O}$  (0.182 g, 1 mmol) and HFur (0.224 g, 2 mmol) were dissolved in MeCN (40 mL). Bpy (0.156 mg, 1 mmol) was added to the resulting suspension, and the reaction mixture was kept at 70°C for 3 h. The blue solution thus formed was filtered and concentrated to a 20 mL volume. After 24 h, blue-colored prismatic crystals were formed; they were separated from the mother liquor by decanting,

washed with MeCN, and dried in air. The yield of I was 0.37 g (80%).

### For $\text{C}_{20}\text{H}_{16}\text{N}_2\text{O}_7\text{Cu}$ (I)

Anal. calcd., %	C, 52.23	H, 3.51	N, 6.09
Found, %	C, 52.17	H, 3.49	N, 6.06

IR ( $\nu$ ,  $\text{cm}^{-1}$ ): 3360 br.w, 3134 w, 3120 w, 3079 w, 3060 w, 3023 vw, 1695 br.w, 1601 m, 1568 vs, 1495 m, 1481 s, 1474 vs, 1447 w, 1385 vs, 1370 vs, 1356 vs, 1322 vw, 1286 w, 1258 w, 1257 w, 1225 m, 1172 m, 1187 vs, 1137 m, 1126 w, 1075 m, 106 m, 1032 vw, 1019 vs, 1007 vs, 928 s, 896 vw, 883 s, 853 w, 812 m, 782 s, 766 vs, 731 m, 663 w, 650 w, 598 br.m, 547 br.m, 468 s.

**Synthesis of  $[\text{Zn}(\text{Fur})_2(\text{Bpy})(\text{H}_2\text{O})]$  (II).** Weighed portions of  $\text{Zn}(\text{OAc})_2 \cdot 2\text{H}_2\text{O}$  (0.219 g, 1 mmol) and HFur (0.224 g, 2 mmol) were dissolved in MeCN (40 mL). Bpy (0.156 mg, 1 mmol) was added to the resulting suspension, and the reaction mixture was kept at 70°C for 3 h. The colorless solution thus formed was filtered and concentrated to a 20 mL volume. After 24 h, transparent needle crystals were formed; they were separated from the mother liquor by decanting, washed with MeCN, and dried in air. The yield of II was 0.32 g (70%).

### For $\text{C}_{20}\text{H}_{16}\text{N}_2\text{O}_7\text{Zn}$ (II)

Anal. calcd., %	C, 52.02	H, 3.49	N, 6.07
Found, %	C, 52.01	H, 3.46	N, 6.03

IR ( $\nu$ ,  $\text{cm}^{-1}$ ): 3156 w, 3114 w, 3077 w, 3058 w, 3023 vw, 1634 w, 1596 vs, 1547 vs, 1474 vs, 1444 m, 1418 vs, 1399 vs, 1318 m, 1256 w, 1229 m, 1178 s, 1159 w, 1072 m, 1056 w, 1026 m, 1010 s, 930 m, 904 w, 884 m, 861 w, 789 s, 771 vs, 734 br.s, 651 m, 634 m, 615 s, 599 s, 546 w.

**Synthesis of  $[\text{Zn}(\text{Fur})_2(\text{Bpy})]$  (III).** Weighed portions of anhydrous  $\text{ZnCl}_2$  (0.136 g, 1 mmol), HFur sodium salt (0.268 g, 2 mmol), and Bpy (0.156 g, 1 mmol) were dissolved in MeCN (40 mL). The resulting suspension was stirred for 24 h at room temperature. Then the reaction mixture was filtered and concentrated to a 10 mL volume with heating (70°C). The resulting solution was kept at room temperature. The precipitated colorless needle crystals were separated from the mother liquor by decanting, washed with MeCN, and dried in air. The yield of III was 0.33 g (74%).

### For $\text{C}_{20}\text{H}_{14}\text{N}_2\text{O}_6\text{Zn}$ (III)

Anal. calcd., %	C, 54.14	H, 3.18	N, 6.31
Found, %	C, 54.09	H, 3.13	N, 6.24

IR ( $\nu$ ,  $\text{cm}^{-1}$ ): 3105 w, 3073 w, 1596 s, 1575 m, 1550 m, 1473 s, 1443 s, 1420 s, 1400 m, 1361 m, 1318 m, 1252 w,

1229 w, 1192 m, 1177 m, 1157 m, 1138 m, 1100 w, 1071 w, 1057 m, 1026 m, 1010 c, 976 w, 930 m, 904 w, 884 w, 884 w, 818 s, 792 s, 769 vs, 732 s, 657 m, 650 m, 635 m, 615 m, 599 m, 479 m, 439 w, 432 w, 414 s.

**Synthesis of  $[\text{Co}(\text{Fur})_2(\text{Bpy})]$  (IV).** Weighed portions of cobalt trimethylacetate (pivalate) (0.261 g, 1.0 mmol), HFur (0.224 g, 2.0 mmol), and Bpy (0.156 g, 1.0 mmol) were placed into a glass tube, and acetonitrile (40 mL) was condensed into the tube. The tube was evacuated, sealed, and heated on an oil bath at 120°C for 2 h. The product crystallized on the tube walls as parallelepiped-shaped violet crystals. The yield of **IV** was 0.43 g (98%).

For  $\text{C}_{20}\text{H}_{14}\text{N}_2\text{O}_6\text{Co}$  (**IV**)

Anal. calcd., %	C, 54.94	H, 3.23	N, 6.41
Found, %	C, 54.89	H, 3.17	N, 6.38

IR ( $\nu$ ,  $\text{cm}^{-1}$ ): 3112 w, 1588 m, 1539 m, 1473 s, 1445 m, 1422 vs, 1367 s, 1316 m, 1230 w, 1194 m, 1177 w, 1158 w, 1070 w, 1056 w, 1025 w, 1009 s, 930 m, 903 m, 884 w, 857 w, 816 s, 791 s, 777 vs, 769 vs, 735 s, 651 w, 635 w, 615 m, 599 m, 531 w, 480 s, 450 w, 415 m.

**X-ray diffraction** study of complexes **I**–**IV** was performed on a Bruker Apex II CCD diffractometer (graphite monochromator,  $\omega$ -scan mode) using  $\text{Cu}K_{\alpha}$  radiation (for **I**, **II**, **IV**) and  $\text{Mo}K_{\alpha}$  radiation (for **III**). The structures were solved with the ShelXT software [20] and refined by the least squares method in the full-matrix anisotropic approximation on  $F_{hkl}^2$  using the Olex2 software [21]. The hydrogen atoms of water molecules in complexes **I** and **II** were located using difference Fourier maps, while positions of other hydrogen atoms were calculated geometrically. All hydrogen atoms were refined in the isotropic approximation by the riding model. The crystallographic data and structure refinement parameters for the complexes are summarized in Table 1 and selective bond lengths are given in Table 2.

The structural data for the complexes are deposited with the Cambridge Crystallographic Data Centre (CCDC noS. 1993168 (**I**), 1993169 (**II**), 1993170 (**III**), 1993171 (**IV**); <http://www.ccdc.cam.ac.uk>).

## RESULTS AND DISCUSSION

The strategy of this study was stemmed from the fact that rational design of bioactive coordination compounds is impossible without understanding the factors governing their interaction with pathogen cells. The nature of the complex forming ion was taken as the variable for elucidating the structure–property–biological activity correlations. We studied a series of biologically important ions: copper(II), zinc(II), and cobalt(II). The complexes  $[\text{M}(\text{Fur})_2(\text{Bpy})(\text{H}_2\text{O})]$  ( $\text{M} = \text{Cu}$  (**I**),  $\text{Zn}$  (**II**)) were prepared by reactions of the acetates  $\text{Cu}(\text{OAc})_2 \cdot \text{H}_2\text{O}$  or  $\text{Zn}(\text{OAc})_2 \cdot 2\text{H}_2\text{O}$  with

HFur ( $\text{M} : \text{Fur} = 1 : 2$ ) followed by addition of Bpy. Mixing of a metal salt with HFur in MeCN gave a suspension, which transformed into a true solution after the addition of Bpy and keeping the reaction mixture at 70°C. It was shown additionally that the simultaneous use of  $\text{ZnCl}_2$  and  $\text{NaFur}$  instead of  $\text{Zn}(\text{OAc})_2 \cdot 2\text{H}_2\text{O}$  by  $\text{ZnCl}_2$  results in the formation of anhydrous complex  $[\text{Zn}(\text{Fur})_2(\text{Bpy})]$  (**III**) in a similar reaction. The complex  $[\text{Co}(\text{Fur})_2(\text{Bpy})]$  (**IV**) was isolated in a similar reaction with the use of a trimethylacetate salt. All of the obtained products were isolated as single crystals, which made it possible to study their structure.

According to X-ray diffraction data, complexes **I** and **II** are isostructural and crystallize in the space group  $P2_1/c$  (Table 1, Fig. 1). (Previously [22–24], isostructural analogues of these complexes differing in the  $\text{M}-\text{N}$  and  $\text{M}-\text{O}$  bond lengths and  $\text{OMO}$ ,  $\text{NMO}$ , and  $\text{NMN}$  bond angles were obtained.) In both cases, the metal cation coordinates two monodentate 2-furoate anions, a chelating Bpy molecule, and a water molecule (Table 2), which form the coordination environment ( $\text{MO}_3\text{N}_2$ ) with a distorted square pyramid geometry ( $\tau_{\text{Cu}} = 0.07$ ,  $\tau_{\text{Zn}} = 0.19$ ) [25]. The hydrogen atoms of the water molecule are involved in the formation of an intramolecular hydrogen bond ( $\text{O} \cdots \text{O}$ , 2.715(4) and 2.653(3) Å;  $\text{OHO}$ , 153(1)° and 146(1)° for **I** and **II**, respectively) with the oxygen atom of one of the anions. A similar intermolecular hydrogen bond ( $\text{O} \cdots \text{O}$ , 2.749(4) and 2.701(3) Å;  $\text{OHO}$ , 152(1)° and 176(1)° for **I** and **II**, respectively) gives rise to infinite hydrogen-bonded chains in the crystals (Fig. 2), which are additionally stabilized by stacking interactions between the centers of the aromatic rings ranging from 3.666(4) to 3.931(4) Å and angles between the planes being 1.78(12)°–3.70(9)°.

In complex **III** (Fig. 3a), the coordination environment of the zinc ion ( $\text{ZnO}_3\text{N}_2$ ) is composed of one chelating Bpy molecule and two (monodentate and chelating) acid anions (Table 2), which corresponds to a distorted square pyramid ( $\tau_{\text{Zn}} = 0.25$ ) [25]. Because of the absence of water molecules in this complex, the infinite chains in the crystal (Fig. 3c) are formed only by stacking interactions between the bipyridine ligands of neighboring molecules with 3.5937(14) Å distance between the centers of aromatic rings and 3.86(8)° angle between the planes of the rings.

Unlike the three previous complexes, the metal ion in **IV** (Fig. 3b) has a pseudo-octahedral coordination environment ( $\text{CoO}_4\text{N}_2$ ), in which both the Bpy molecule and both 2-furoate anions are bidentate ligands (Table 2). In this case, too, the major structural motif in the crystal (Fig. 3d) is formed by infinite chains consisting of molecules of the complex connected by stacking interactions between the bipyridine ligands, with the distance between the centers of aromatic rings

**Table 1.** Crystallographic data and structure refinement details for complexes **I**–**IV**

Parameter	Value			
	<b>I</b>	<b>II</b>	<b>III</b>	<b>IV</b>
<i>M</i>	459.90	461.72	443.739	437.26
<i>T, K</i>	120	120	120	120
System	Monoclinic	Monoclinic	Monoclinic	Monoclinic
Space group	<i>P</i> 2 <sub>1</sub> / <i>c</i>	<i>P</i> 2 <sub>1</sub> / <i>c</i>	<i>P</i> 2 <sub>1</sub> / <i>n</i>	<i>P</i> 2 <sub>1</sub> / <i>n</i>
<i>Z</i>	4	4	4	4
<i>a</i> , Å	6.935(3)	6.7989(5)	7.1783(2)	7.2429(6)
<i>b</i> , Å	16.746(7)	16.9370(14)	15.9764(3)	16.1854(12)
<i>c</i> , Å	16.422(7)	16.2927(12)	15.9478(3)	16.0247(12)
β, deg	97.448(10)	96.063(2)	97.015(1)	96.535(3)
<i>V</i> , Å <sup>3</sup>	1891.1(14)	1865.7(2)	1815.26(7)	1866.4(3)
ρ(calcd.), g cm <sup>-3</sup>	1.6152	1.644	1.624	1.556
μ, cm <sup>-1</sup>	12.03	13.65	22.63	9.10
<i>F</i> (000)	942	944	901	892
2θ <sub>max</sub> , deg	60	50.5	135	60
Number of measured reflections	10 605	14 289	24 797	18 002
Number of unique reflections ( <i>R</i> <sub>int</sub> )	5527 (0.696)	4489 (0.0692)	3199 (0.0905)	4121 (0.1218)
Number of reflections with <i>I</i> > 2σ( <i>I</i> )	4231	3286	2798	2119
Number of refined parameters	272	271	262	262
<i>R</i> <sub>1</sub> , <i>wR</i> <sub>2</sub> ( <i>I</i> > 2σ( <i>I</i> ))	0.0526, 0.1030	0.0423, 0.0833	0.0362, 0.0799	0.0740, 0.1285
<i>R</i> <sub>1</sub> , <i>wR</i> <sub>2</sub> (all data)	0.0817, 0.1126	0.0670, 0.0946	0.0433, 0.0842	0.1599, 0.1567
GOOF	1.0497	1.011	1.0573	1.064
Δρ <sub>min</sub> /Δρ <sub>max</sub> , e Å <sup>-3</sup>	-0.869/0.792	-0.575/0.387	-0.471/0.320	-0.439/0.340

**Table 2.** Selected bond lengths (Å) and angles (deg) for **I**–**IV**

Bond	<b>I</b>	<b>II</b>	<b>III</b>	<b>IV</b>
	<i>d</i> , Å			
M–O(Fur)	1.973(3), 1.984(3)	2.0275(19), 2.0467(19)	1.9875(18), 2.1035(18), 2.2063(17)	2.020(4), 2.098(4), 2.198(4), 2.316(3)
M–O(H <sub>2</sub> O)	2.222(3)	2.0245(19)		
M–N	2.016(3), 2.025(2)	2.096(2), 2.156(2)	2.0790(19), 2.092(2)	2.075(4), 2.080(4)
OMO	91.01(10)–97.18(10)	92.62(8)–101.77(8)	61.35(7), 92.65(7), 111.08(7), 142.64(7)	60.42(15), 61.50(14), 96.28(14), 99.76(15), 146.75(15)
Angle	ω, deg			
NMO	91.52(11)–98.83(10), 162.94(11), 167.40(11)	89.35(8)–105.06(8), 151.92(8), 163.06(8)	96.51(7)–109.18(7), 157.93(7)	94.77(15)–108.20(15), 159.26(16), 163.10(15)
NMN	80.22(12)	76.61(9)	79.04(7)	78.74(16)

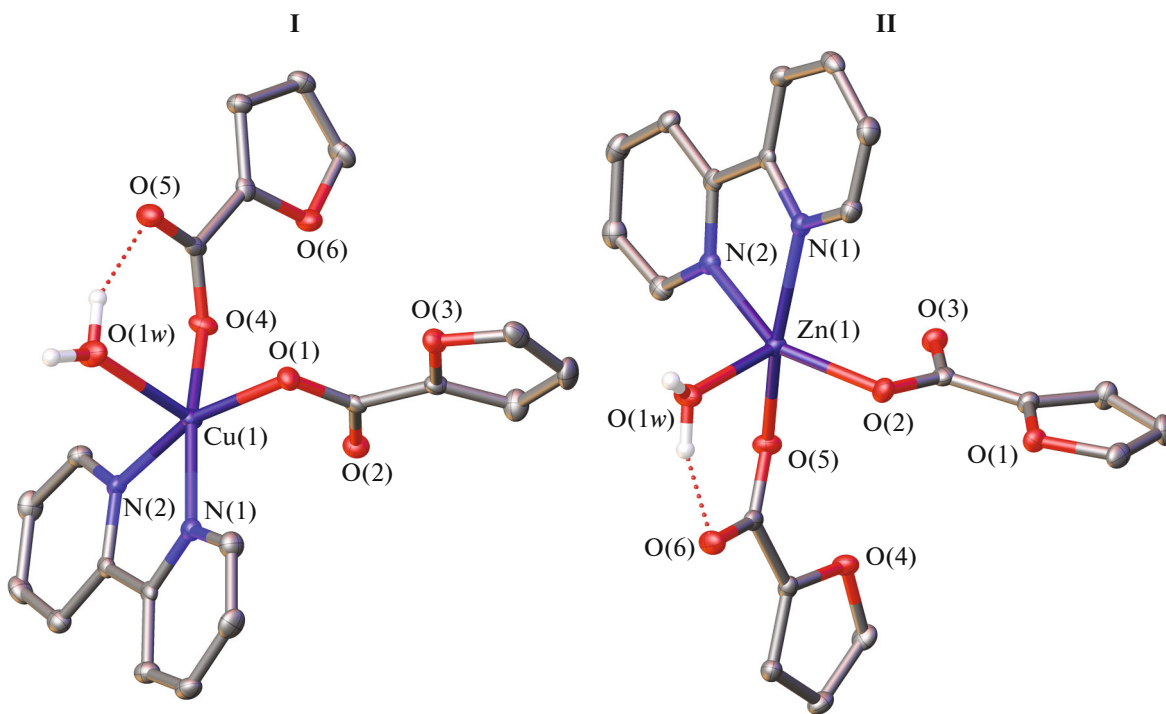


**Fig. 1.** Molecular structure of complexes **I** and **II**. Here and below the atoms are drawn as thermal ellipsoids ( $p = 50\%$ ). The hydrogen atoms (except those of water molecules) are omitted for clarity.

being  $3.907(3)$  Å and the angle between the planes being  $3.43(18)$ °.

The antibacterial activity of compounds **I**, **III**, and **IV** was assessed against the nonpathogenic *M. smegmatis* strain. It is known that the chemotherapeutic drug resistance of mycobacteria is due to low permeability and unusual structure of the mycobacterial cell wall. *M. smegmatis* are rapidly growing nonpathogenic bacteria and, therefore, they are used to model the slowly growing *M. tuberculosis* and for the primary screening of antituberculosis drugs [26]. The *M. smegmatis* test system has a higher antibiotic and antituberculosis drug resistance than *M. tuberculosis*; therefore, the compound concentration of  $<100$  nmol/disc served as the selection criterion, unlike *M. tuberculosis* [27]. The test method included determination of the diameter of growth inhibition zone for the *M. smegmatis* culture, grown as a lawn on an agarized medium around paper discs impregnated with test compounds. The compounds were deposited on the discs in various concentrations. The halo (growth inhibition zone) diameter was found to increase with increasing amount of the compound deposited on the disc. Concentration of the compound producing the minimum visible growth inhibition zone was taken as the MIC (μg/disc). The results of antibacterial activity assays in the *M. smegmatis* mc<sup>2</sup> 155 test system and its variation with time for compounds **I**, **III**, and **IV** are summarized in Table 3. As follows from the data of Table 3, the biological activity of compounds **I** and **III** is

~2 times higher than that of isoniazid and is slightly lower than that of rifampicin. Despite the fact that free Bpy exhibits a low biological activity, the activity markedly increases for complexes **I** and **III** (a similar effect was observed previously [19]). In addition, the inhibition zone detected for free Bpy in the first 24 h of culture growth is entirely overgrown after 5 days (indicating a weak bacteriostatic action of Bpy), whereas the activity of **I** against the bacteria remains the same even after 5 days. For complex **III**, like for free Bpy, the viability of the bacteria is completely restored after 5 days.

Thus, copper(II), zinc(II), and cobalt(II) ions with 2-furoate anions and Bpy form mononuclear isostructural complexes. The structures are stabilized by hydrogen bonds (**I** and **II**) and by stacking interactions between bipyridine ligands (all complexes). It is evident that the nature of the complexing ion determines the biological activity of complexes. Compounds **I** and **III** show identical biological activities in vitro against *M. smegmatis*. However, the high activity of complex **I** does not change with time and, therefore, this compound may be promising for testing against the virulent *M. tuberculosis* strain.

#### CONFLICT OF INTEREST

The authors declare that they have no conflicts of interest.

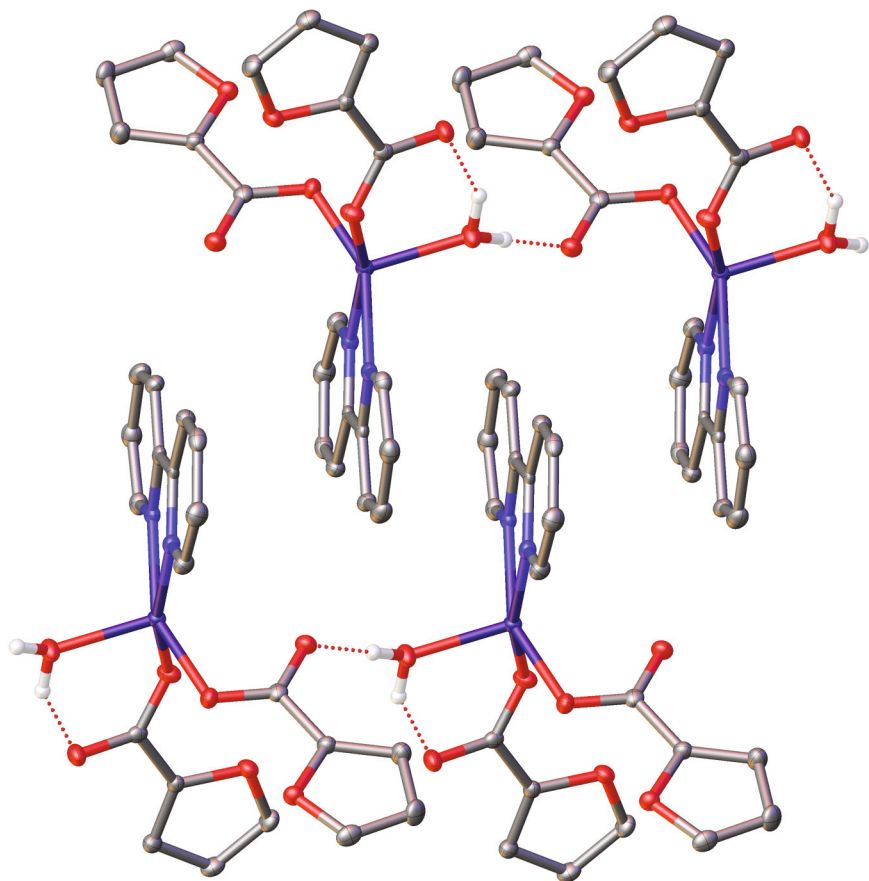


**Fig. 2.** Fragment of packing of the complexes in the crystals of **I** and **II**, illustrating the formation of hydrogen-bonded chains (the hydrogen atoms are shown by dashed line).

#### ACKNOWLEDGMENTS

The X-ray diffraction studies were supported by the Ministry of Science and Higher Education of the Russian Federation and performed using research equipment of the Center of Investigation of Molecular Structure of the Nesmeyanov Institute of Organoelement Compounds,

Russian Academy of Sciences. Elemental analysis and IR spectroscopy were carried out using research equipment of the Center for Collective Use of the Physical Investigation Methods, Kurnakov Institute of General and Inorganic Chemistry, Russian Academy of Sciences, which was supported by the State Assignment for the Kurnakov Institute

**Table 3.** Results of antibacterial activity assays against *Mycobacterium smegmatis*

Compound	MIC, ( $\mu\text{g}/\text{disc}$ )	Growth inhibition zone for <i>M. smegmatis</i> mc <sup>2</sup> 155, mm	
	24 h	24 h	120 h*
<b>I</b>	46	7.0	7.0
<b>III</b>	44	6.5	0
<b>IV</b>	175	6.5	6.5
HFur	112	6.5	
INH	100	9.0	6.5
RMP	10	7.0	7.0
Bpy	78	7.5	

\* The diameter of culture growth inhibition zone does not change over this period of time; the empty cell means that the growth inhibition zone is absent.

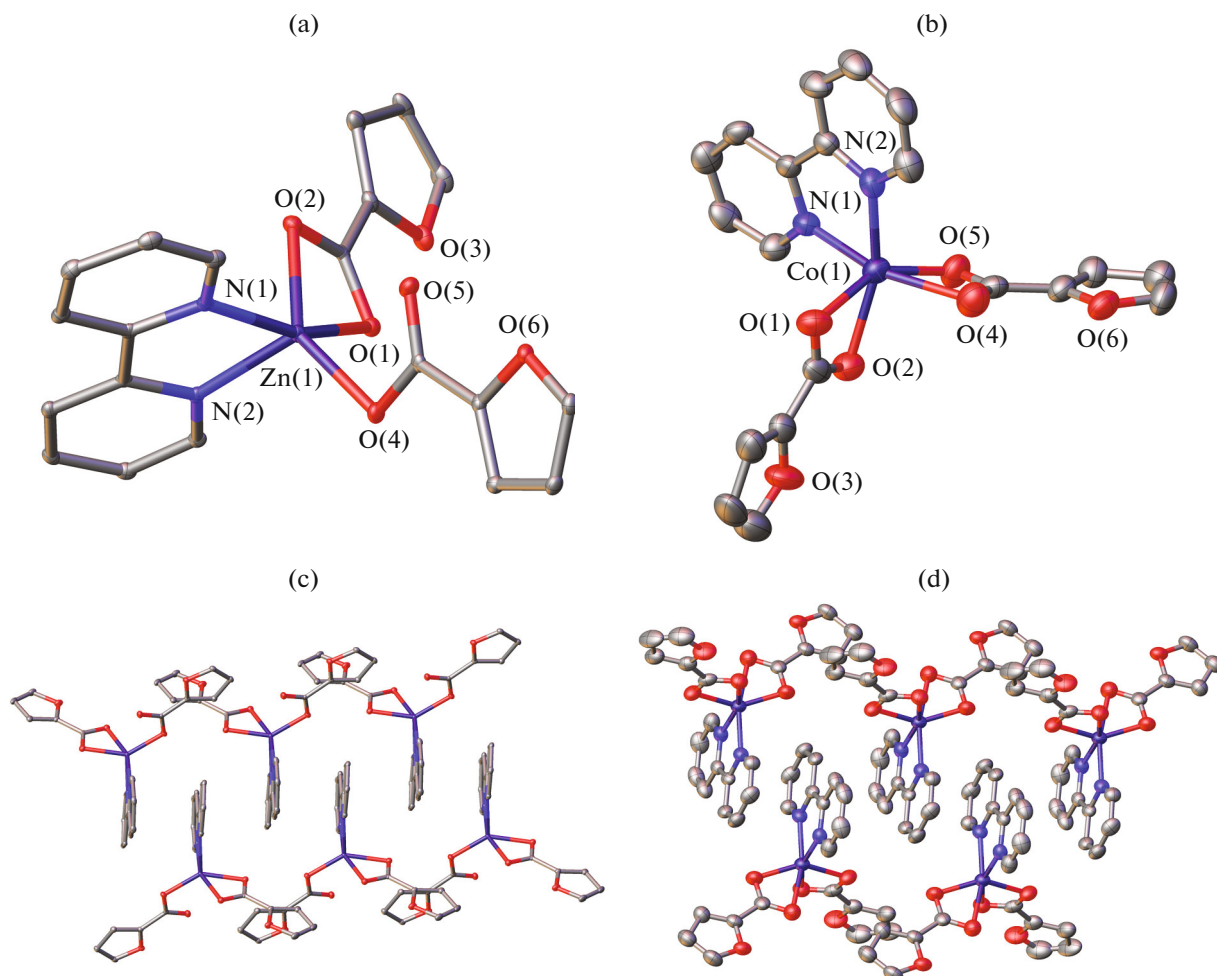


**Fig. 3.** Molecular structure of complexes (a) **III** and (b) **IV** and (c, d) fragments of their packing in the crystal, illustrating the formation of infinite chains via stacking interactions, respectively.

of General and Inorganic Chemistry, Russian Academy of Sciences, in the field of fundamental research.

#### FUNDING

This work was supported by the Russian Science Foundation (project 20-13-00061).

#### REFERENCES

1. Louie, A.Y. and Meade, T., *J. Proc. Natl. Acad. Sci. USA*, 1998, vol. 95, p. 6663.
2. Rojas, S., Quartapelle-Procopio, E., Carmona, F.J., et al., *J. Mater. Chem. B*, 2014, vol. 2, p. 2473.
3. Thompson, K.H. and Orvig, C.J., *Inorg. Biochem.*, 2006, vol. 100, p. 1925.
4. Bello-Vieda, N., Pastrana, H., Garavito, M., et al., *Molecules*, 2018, vol. 23, p. 361.
5. Goodwin, L., *Am. J. Trop. Med. Hyg.*, 1995, vol. 89, p. 339.
6. *Global Tuberculosis Report 2018*, Geneva: World Health Organization, 2018.
7. Mjos, K.D. and Orvig, C., *Chem. Rev.*, 2014, vol. 114, p. 4540.
8. Rosenberg, B., VanCamp, L., and Krigas, T., *Nature*, 1965, vol. 205, p. 698.
9. Rosenberg, B., VanCamp, L., Trosko, J.E., and Mansour, V.H., *Nature*, 1969, vol. 222, p. 385.
10. Alderden, R.A., Hall, M.D., and Hambley, T.W.J., *J. Chem. Educ.*, 2006, vol. 83, p. 728.
11. Berners-Prie, S.J., Ronconi, L., and Sadler, P.J., *Prog. Nucl. Magn. Reson. Spectrosc.*, 2006, vol. 49, p. 65.
12. Cleare, M.J. and Hoeschele, J.D., *Bioinorg. Chem.*, 1973, vol. 2, p. 187.
13. Cleare, M.J. and Hoeschele, J.D., *Platinum Met. Rev.*, 1973, vol. 17, p. 2.
14. Gibaud, S., Jaouen, G., and Jaouen, G., *Med. Organometall. Chem.*, 2010, p. 1.
15. Patra, M., Gasser, G., and Metzler-Nolte, N., *Dalton Trans.*, 2012, vol. 41, p. 6350.

16. Ovchinnikov, Yu.A., *Bioorganicheskaya khimiya* (Bio-organic Chemistry), Moscow: Prosveshchenie, 1987.
17. Krátk, M., and Vinová, J., *Curr. Med. Chem.*, 2012, vol. 19, p. 6126.
18. Melnic, S., Prodius, D., Stoeckli-Evans, H., et al., *Eur. J. Med. Chem.*, 2010, vol. 45, p. 1465.
19. Lutsenko, I.A., Baravikov, D.E., Kiskin, M.A., et al., *Russ. J. Coord. Chem.*, 2020, vol. 46, no. 6, p. 411. <https://doi.org/10.1134/S1070328420060056>
20. Sheldrick, G.M., *Acta Crystallogr., Sect. A: Found. Adv.*, 2015, vol. 71, p. 3.
21. Dolomanov, O.V., Bourhis, L.J., Gildea, R.J., et al., *J. Appl. Crystallogr.*, 2009, vol. 42, p. 339.
22. Zheng, X., Zhou, Y., Zhang, H., et al., *Synth. React. Inorg. Metal-Org. Nano-Metal Chem.*, 2007, vol. 37, p. 235.
23. Zheng, X., Shen, X., Wan, X., et al., *J. Coord. Chem.*, 2007, vol. 60, p. 1317.
24. Ai, Ch., Xiang, J., Li, M., et al., *Acta Crystallogr., Sect. E: Struct. Rep. Online*, 2007, vol. 63, p. m565.
25. Addison, A.W. and Rao, T.N., *J. Chem. Soc., Dalton Trans.*, 1984, p. 1349.
26. Ramon-Garcia, S., Ng, C., Anderson, H., et al., *Antimicrob. Agents. Chemother.*, 2011, vol. 8, p. 3861.
27. Bekker, O.B., Sokolov, D.N., Luzina, O.A., et al., *Med. Chem. Res.*, 2015, vol. 24, p. 2926.

*Translated by Z. Svitanko*